

# Electronic states and charge-transfer mechanisms in solid molecular hydrogen

Efthimios Kaxiras<sup>a,\*</sup>, Jeremy Broughton<sup>b</sup>

<sup>a</sup> *Department of Physics and Division of Applied Sciences, Harvard University, Cambridge, MA 02138, USA*

<sup>b</sup> *Complex System Theory Branch, Naval Research Laboratory, Washington, D.C. 20375, USA*

Received 20 January 1994; accepted 3 March 1994

---

## Abstract

Metallic behavior and the transition from a molecular to an atomic phase in solid hydrogen under pressure have been predicted theoretically and sought after experimentally for a long time. We report extensive first-principles investigations of the electronic states in static, hexagonal close packed (hcp) structures which are representative of solid molecular hydrogen at high pressure. In a structure which preserves the full hcp symmetry, charge is transferred from bonding to antibonding states at pressures near 1.5 Mbar. However, at still higher pressure charge transfer takes place in the opposite direction. In a different structure of lower symmetry and lower energy, antibonding states do not become occupied until much higher pressure ( $\sim 2.5$  Mbar). The character of antibonding electronic states and their occupation with pressure provide insight into possible metallic behavior and the transition to the atomic phase.

---

## 1. Introduction

The prediction of Wigner and Huntington [1] that at sufficiently high pressure the ground state of hydrogen will be an atomic, metallic solid has provided the impetus for much theoretical and experimental work. Ashcroft recognized that the atomic phase would be a superconductor [2], and detailed calculations for the critical temperature of this phase gave values near room temperature [3,4]. Achieving the necessary conditions to observe this phase has been the subject of intense experimental work. At low pressure and low temperature solid hydrogen is a wide band-gap insu-

lator, consisting of  $H_2$  molecules pinned on a hcp lattice [5,6]. The atoms are strongly bonded in pairs forming  $H_2$  molecular units with intra-pair distances close to the bond length of free  $H_2$  molecules (1.4 a.u.), and inter-pair separations considerably larger. The atomic motions in the solid can be described in terms of intra-molecular vibrations with a frequency close to that of free molecules ( $\sim 4000\text{ cm}^{-1}$ ) and inter-molecular vibrations akin to lattice phonon modes, with frequencies that depend strongly on the pressure (reaching  $\sim 1000\text{ cm}^{-1}$  at 1.5 Mbar) [7,8]. In addition, individual  $H_2$  units in the solid undergo rotational motion, which at very low pressure is similar to quantum rotational states of free  $H_2$  molecules [9]. As the inter-molecular interactions increase with pressure, the free-molecule eigen-

---

\* Corresponding author.

states are no longer good quantum numbers for the rotational motion in the solid, which becomes rather complex [7]. Some of these features survive to the very high pressure of 1.5 Mbar.

At still higher pressure, intra- and inter-molecular distances start to become comparable and, consequently, the frequencies of molecular vibrations and of lattice phonon modes are no longer uncoupled [10]. Eventually, the  $H_2$  units should break down and transform to the Wigner–Huntington atomic phase. Several experimental reports of metallic-like behavior in the neighborhood of 1.5 Mbar [11,12] seem to support theoretical expectations [13,14] that electrons become delocalized in the solid even before the molecular bonds break down. The experimental observations of metallic behavior have been challenged by subsequent work [15,16]. At present, the nature of the metallic state and even its existence remain controversial [17]. Recent theoretical investigations have underscored the importance of quantum motion of the protons [18], which makes it difficult to describe this system in terms of the traditional language of solids, that is, electron energy bands.

This paper attempts to elucidate some aspects of the behavior of solid hydrogen in the pressure range 1–2 Mbar. We have calculated the distribution of electronic charge in representative structures for a range of densities, and have examined possible charge-transfer mechanisms. We also examined the nature of individual electron wavefunctions, the occupation of which could lead to metallic behavior or to molecular dissociation. Our results give a detailed description of electronic behavior both in reciprocal space (spanned by the wave-numbers  $\mathbf{k}$  of electrons) and in real space. Some interesting features are found, which provide new insight into the behavior of this complex quantum solid.

## 2. Structure of molecular hydrogen

First and foremost, one needs to establish a realistic picture for the structure of the molecular phase at high pressure. While this remains a daunting task due to quantum motions of the

protons, several structures have been proposed as low-energy configurations for this pressure range. Kaxiras et al. showed that a class of static structures with the molecular axes inclined by  $60^\circ$  off the  $c$ -axis of the hcp lattice have in general low energy and wide indirect band-gaps in the spectrum of electronic states [19]. Nagara and Nakamura [20] found a structure in the same class (i.e. with molecules tilted away from the  $c$ -axis), which has lower energy than the structures of Ref. [19]. Structures of still lower energy and lower symmetry cannot be excluded. By contrast, a static structure first discussed by Abrikosov [21] with the molecules oriented along the  $c$ -axis, has the highest energy and the smallest indirect band-gap among all the structures we considered. The rather large zero-point quantum-mechanical proton motion implies that a range of structures *both in molecular orientations and in intra-pair separations* are accessible to the system, even at  $T=0$  K. In free hydrogen molecules, the energy associated with zero-point motion is  $\sim 0.25$  eV. Within a semiclassical picture, a particle with this energy in a harmonic well has a turning point radius which translates to molecular bond-length deviations of  $\pm 15\%$ . Both the energy and the bond-length deviations due to zero-point motion are different in the solid. Energy differences due to changes of molecular orientation in the solid, in the pressure range 1–1.5 Mbar, are of order 0.05 eV per molecular [19]. These order-of-magnitude comparisons suggest that several static structures should be investigated in order to glean the behavior of the real solid.

Here, we report on extensive calculations of electronic states associated with the lowest- and highest-energy static structures within a primitive hcp unit cell. Our calculations are based on the Kohn–Sham formulation of density functional theory, using the local density approximation (DFT/LDA) to describe electronic exchange-correlation effects [22]. This is a quantum-mechanical parameter-free approach that describes accurately the electronic density and relative energy. In order to capture the details of electronic charge distribution we use a plane-wave basis which includes plane waves with kinetic energy up to 100 Ry and 144 uniformly spaced points in

the full Brillouin zone for reciprocal-space integrations. The two structures we will discuss in detail were chosen among the many we have considered as representative of the range of configurations available to the system. The highest-energy structure (H- $\alpha$ ) has all the molecular axes oriented along the  $c$ -axis of the hcp lattice. The lowest energy one (H- $\gamma$ ) has the molecular axes tilted off the  $c$ -axis by  $60^\circ$  with their projections on the  $ab$ -plane bisecting the angles between the planar lattice vectors. Molecules in alternate planes are tilted in opposite directions, i.e. their azimuthal angles differ by  $180^\circ$ . This type of arrangement allows molecules to maximally avoid each other.

In Fig. 1 we present charge-density distributions for the two structures. The bond length in both structures is kept fixed at the value of 1.4 a.u. The molecular density at which this calculation was performed is 6.96 times higher than the density of the solid at atmospheric pressure ( $d_0 = 0.043478 \text{ mol/cm}^3$ ). Using an equation of state based on extrapolation of low-pressure experimental measurements [23], this molecular density translates to a pressure of 0.75 Mbar. This value of the pressure should be taken only as an estimate, since the calculation was based on static structures, whereas the experimental measurements include the full range of proton motions. The charge density plots of Fig. 1 give a clear sense of the electronic distribution in the system and provide a visualization of the statement made above with respect to molecules maximally avoiding each other in the H- $\gamma$  structure.

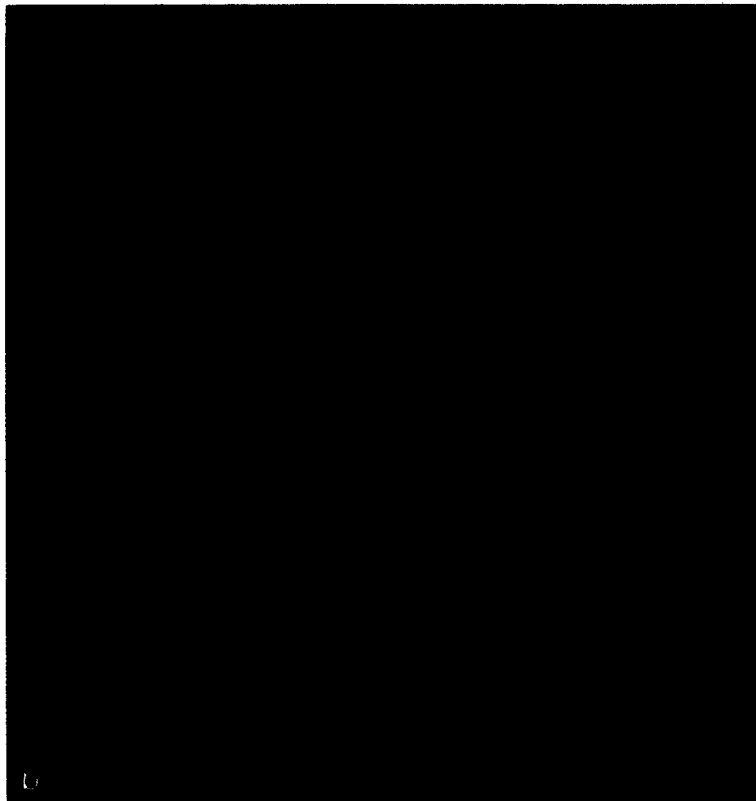
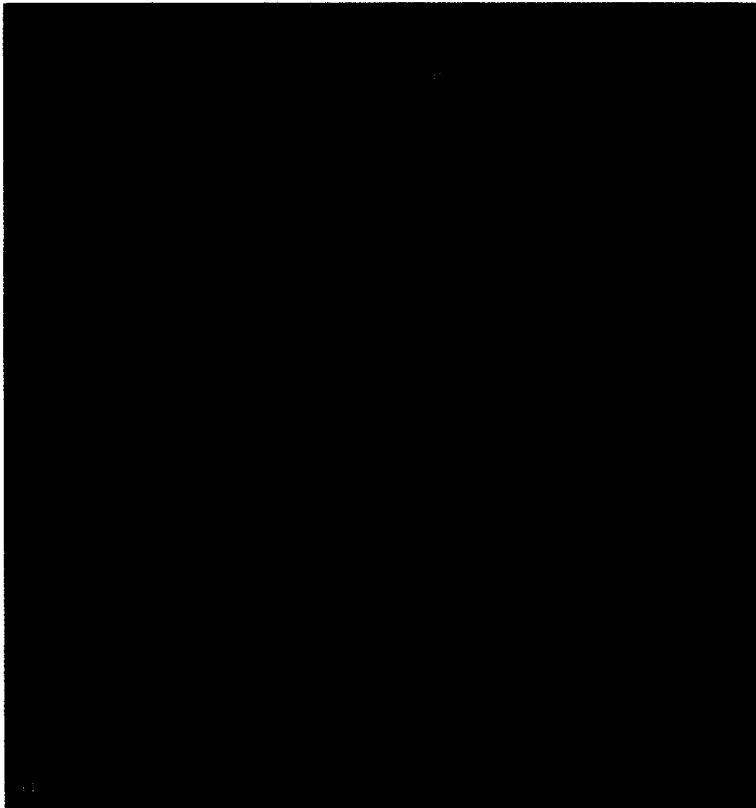
### 3. Electronic states in molecular hydrogen

The electronic energy bands for the H- $\alpha$  and H- $\gamma$  configurations at a density  $d/d_0 = 6.96$  are shown in Fig. 2. At this molecular density, both structures are insulating, that is, states below the

Fermi level (bonding states) are separated by an energy gap from states above the Fermi level (antibonding states). When discussing electronic band gaps one should bear in mind that the approach we are using here tends to underestimate the separation between occupied and unoccupied states in an insulating crystal, but gives an accurate description of their dispersion in reciprocal space (see Refs. [24–26] for more extensive discussion). There are two important differences between the band structures of the H- $\alpha$  and H- $\gamma$  structures: First, the H- $\gamma$  structure has a much larger band gap, and second, the lowest antibonding state shifts from the center of the Brillouin zone ( $\Gamma$  point) in the H- $\alpha$  structure to a point on the surface of the Brillouin zone in the H- $\gamma$  structure (K point, with  $k_z = \pi/c$ ). Less significant changes in the energy of occupied states can also be seen in Fig. 2. For instance, the position of the highest occupied state is slightly different for the two band structures, but remains in the same general direction in the Brillouin zone. We emphasize that, due to zero-point motion, the real solid is not described accurately by either band structure, but the electronic states associated with the H- $\alpha$  and H- $\gamma$  structures should be representative of the accessible range due to rotational motion, while bond-length variations change the energy scale.

We consider next the effect of pressure on the electronic states. It has been proposed that at higher pressure the bonding and antibonding states of the molecules in the hcp crystal will start overlapping in energy [24–26]. In Fig. 3 we show the behavior of the band gap for the H- $\alpha$  and H- $\gamma$  structures as a function of increasing density (and pressure). Within our DFT/LDA based approach the band gaps decrease linearly with increasing density. The linear behavior is somewhat changed when many-body effects are included in the quasiparticle energies [26], but the overall trends remain essentially unchanged. The gap for

Fig. 1. Charge density distributions for the (a) H- $\alpha$  and (b) H- $\gamma$  structures. The white dots represent the positions of the protons. Isosurfaces corresponding to the same electronic density value are shown in the same color. Notice that the blue isosurface is continuous in (a), i.e. neighboring molecules “touch” each other; in (b), the same isosurface is broken in regions associated with individual molecules, i.e. molecules “avoid” one another.



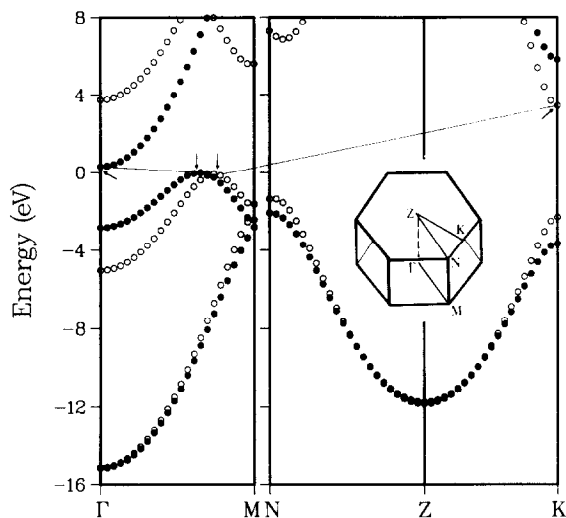


Fig. 2. Energy bands corresponding to the H- $\alpha$  (filled dots) and the H- $\gamma$  (open dots) structures at relative density  $d/d_0 = 6.96$ . The states below the Fermi level (0 of energy) correspond to bonding states, the higher energy ones to antibonding states. The arrows indicate the positions of the highest occupied bonding states and the lowest unoccupied antibonding ones. Thin diagonal lines show the indirect band gap. The inset is a schematic view of the Brillouin zone, with high symmetry points identified.

the H- $\alpha$  structure closes much earlier with increasing pressure, indicating a tendency of this structure to exhibit metallic behavior easily. By contrast, a considerably larger pressure is required to induce gap closure in the lower energy H- $\gamma$  structure.

#### 4. Charge-transfer effects

The closing of the band gap is expected to be accompanied by charge transfer from the highest occupied bonding states to the lowest unoccupied antibonding states. This charge transfer will affect the intra-molecular vibrational frequency as the molecular bonds are weakened when they are depleted of electronic charge. It could also signal the onset the metallic behavior due to occupation of antibonding states which are usually more extended. In order to investigate the charge-transfer mechanisms we have calculated the electronic charge distribution at molecular densities ranging from  $d/d_0 = 6.96$  to 9.87 (corresponding to pres-

ures that range from 0.75 to 1.80 Mbar) [23]. The results are displayed in Figs. 4(a) and (b), for the two structures. The upper panel in each case shows the charge density along the axis of a molecule at the lowest molecular density ( $d/d_0 = 6.96$ ); the lower panel shows the *difference* in charge density with respect to the upper panel, as the density increases. The asymmetry in charge-density distribution along the molecular bond in Fig. 4(b) is due to the lower symmetry of the H- $\gamma$  structure. The most prominent feature in the charge-density differences of both structures is an increase of electron concentration near the position of the protons (at  $\pm 0.7$  a.u.).

When a significant amount of charge is transferred from bonding to antibonding states, the charge-density difference should take on negative values in the center of the molecular bond, where the antibonding states have a node. In the H- $\alpha$  structure, at the molecular density of  $d/d_0 = 7.89$ , the charge-density difference is positive, even though the gap between bonding and antibonding

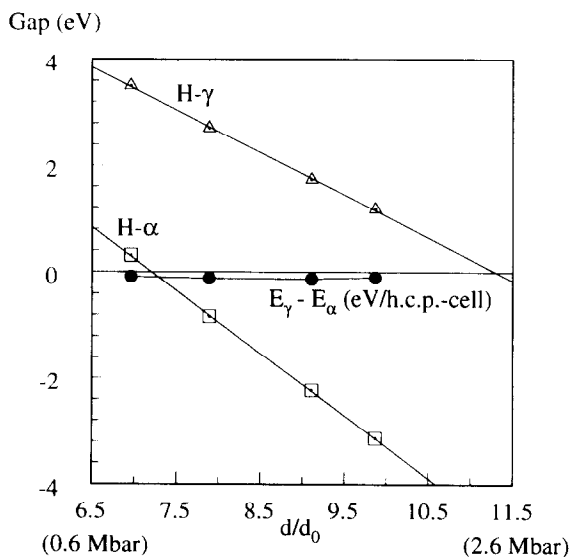


Fig. 3. Minimum gap in the electronic spectrum as a function of density for the H- $\alpha$  (squares) and H- $\gamma$  (triangles) structures (the corresponding pressure range from Ref. [23] is also shown). The points are calculated values; lines are fits. A negative gap indicates the range of overlap between bonding and antibonding states. The total-energy difference between the two structures is also shown (solid dots) in eV per hcp unit cell.

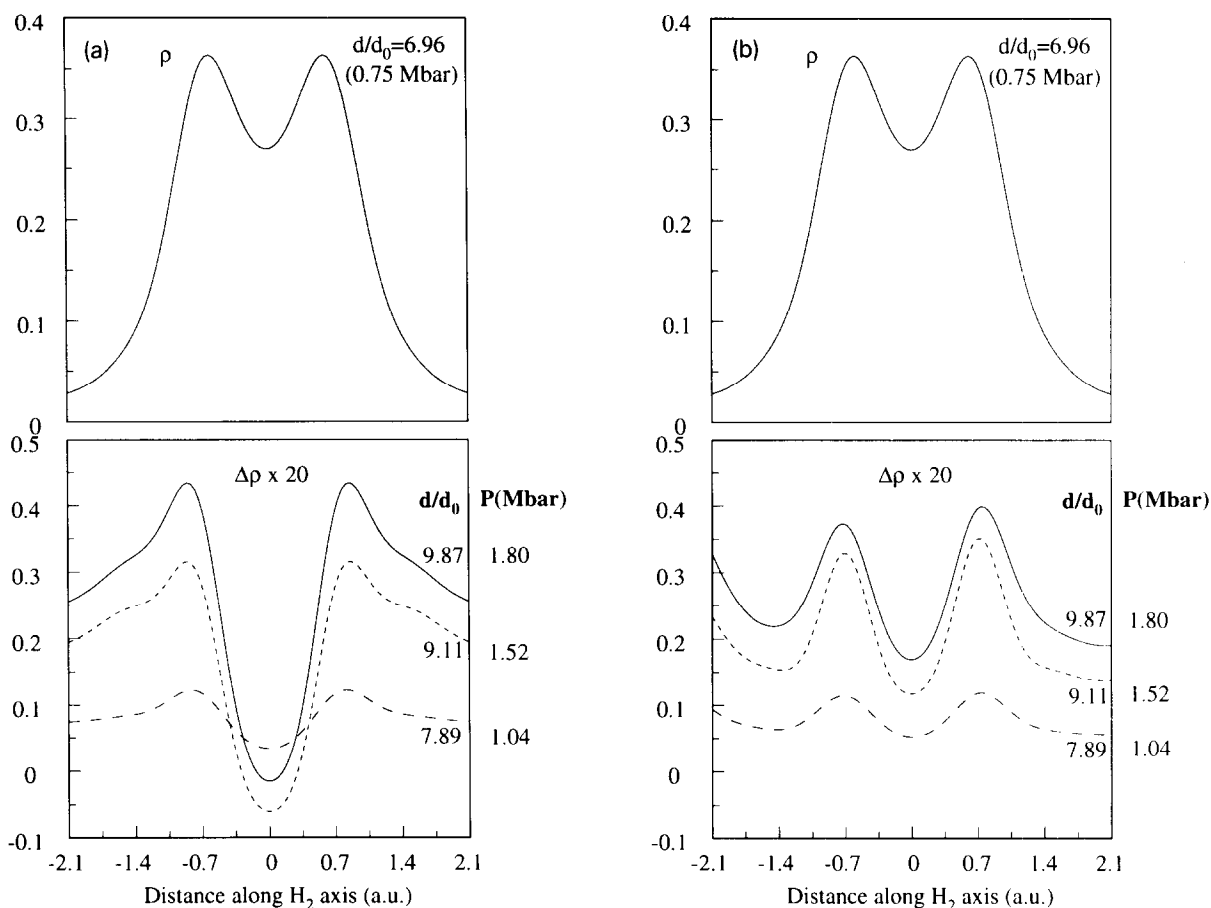


Fig. 4. Charge density (upper panels) and charge-density differences (lower panels) along a molecular axis in (a) the  $H-\alpha$  and (b)  $H-\gamma$  structures, in atomic units. The charge-density differences are multiplied by a factor of 20 to bring them to the same scale as the charge density itself. The values of the density  $d/d_0$  are shown. Corresponding pressure values obtained from the experimental equation of state (Ref. [23]) are also given.

states has vanished (see Fig. 3). This clearly indicates that despite the vanishing of the electronic band gap, the occupation of antibonding states is not adequate to deplete the molecular bond of electronic charge. The charge-density difference develops a negative dip at  $d/d_0 = 9.11$  near the center of the molecule. It is noticeable how small the amount of charge transfer actually is. The charge-density difference is less negative over a smaller region of space at molecular density  $d/d_0 = 9.87$ . These results indicate that as the density increases beyond  $d/d_0 = 9.11$ , the occupation of antibonding states is actually *reduced*. This surprising result can be understood by a closer look at the band structure (Fig. 2): The increase of the

pressure brings about the expected charge transfer from bonding to antibonding states as the two sets of energy bands start overlapping. At still higher pressure, however, the strong upward dispersion of antibonding states leads to a smaller rate of filling relative to bonding states, which have little dispersion near the maximum.

In contrast to all this, the charge-density difference for the  $H-\gamma$  structure never becomes negative (Fig. 4(b)). This can also be interpreted in terms of band-structure features: In the pressure range considered here the gap between bonding and anti-bonding states for the  $H-\gamma$  structure never vanishes, as shown in Fig. 3. Furthermore, the upward dispersion of low-lying antibonding



states at the Brillouin zone surface ( $k_z = \pi/c$ ) is much sharper in the H- $\gamma$  structure (Fig. 2). Thus, even when the band gap vanishes in this structure, which occurs in the neighborhood of 2.5 Mbar (see Fig. 3), there are very few antibonding states available for charge transfer due to their sharp dispersion. As a consequence, it is more difficult to deplete the bond of electronic charge in the H- $\gamma$  structure, which implies that much higher pressure would be required to dissociate molecules in this structure.

A final interesting feature is the behavior of the charge density in the inter-molecular regions. Charge is transferred to these regions mostly through occupation of antibonding states, which have a large amplitude outside the molecular bond. This is exhibited by the large values of the charge-density differences in the “wings” of Fig. 4(a). The spatial distribution of charge in the inter-molecular regions will have important ramifications for the nature of the transition to the atomic phase. To shed light on this matter, we present in Fig. 5 three-dimensional plots of the amplitude of the wavefunction for the lowest antibonding state of the H- $\alpha$  and H- $\gamma$  structures (the location of these electronic states in the Brillouin zone is identified in Fig. 2). There is a striking *qualitative difference* between the two wavefunctions: In the H- $\alpha$  structure, the wavefunction has strong two-dimensional character, with large amplitude in hexagonal planar lobes (Fig. 5(a)). In the H- $\gamma$  structure, on the other hand, the character of the wavefunction is closer to one-dimensional, with large amplitude along tubes (Fig. 5(b)). If the H- $\gamma$  class of structures is dominant, the molecules will dissociate via linear chains, whereas if the H- $\alpha$  class of structures were to dominate, molecular dissociation would proceed via planar arrangements. Recently, Hohl et al. [27] have described such changes in the dimensionality of the system found by molecular-dynamics simulations.

## 5. Discussion and conclusions

Let us briefly discuss the implications of our results for possible metallic behavior in the neighborhood of 1.5 Mbar. This could occur if a significant portion of the molecules were to assume the H- $\alpha$  structure. For static configurations, this arrangement is energetically unfavorable: the H- $\gamma$  structure is lower in energy than the H- $\alpha$  structure throughout the range of densities considered (by 0.09, 0.12, 0.13, 0.10 eV/hcp unit cell, at densities  $d/d_0 = 6.96, 7.89, 9.11, 9.87$ , respectively, see Fig. 3). The large zero-point motion, however, could allow parts of the system to attain structures similar to H- $\alpha$ . This effect would populate locally antibonding states, which could give rise to metallic-like features. The nature of this metallic state will be different from a typical band metal (i.e. the Drude model), and might be related to percolation or hopping conductivity. This type of metallic behavior could explain apparent inconsistencies in attempts to relate measurements of absorption and reflection through a Drude model [15,17].

To conclude, we have presented detailed comparisons of electronic states and charge-density distributions in two representative hcp structures of molecular solid hydrogen in the pressure range between 0.75 and 1.8 Mbar. The comparisons reveal unexpected behavior in the charge-transfer mechanisms. Specifically, in the high-symmetry (and higher energy) H- $\alpha$  structure charge is transferred from bonding to antibonding states in the density range  $d/d_0 \sim 9$ , and back to bonding states at higher density; in the low-symmetry (and lower energy) H- $\gamma$  structure, antibonding states never become occupied in this pressure range, and the gap in the electronic spectrum does not vanish to much higher pressure ( $\sim 2.5$  Mbar). Finally, the wavefunctions of the lowest antibonding state in the two structures were compared and shown to have a qualitatively different behav-

Fig. 5. Amplitude of the lowest antibonding state wavefunction for the (a) the H- $\alpha$  and (b) the H- $\gamma$  structures. Isosurfaces of the same value are shown in the same color. White dots indicate the proton sites. Notice the predominance of two-dimensional lobes in (a) and one-dimensional tubes in (b).

ior. Implications for the nature of a possible metallic state and the transition to the atomic phase were discussed.

### Acknowledgements

We wish to acknowledge helpful comments and discussions with I.F. Silvera, and thank R.J. Hemley for providing an English translation of Ref. [21]. The assistance of D.W. Hess in producing the color figures is gratefully acknowledged. The calculations were performed at the Pittsburgh Supercomputer Center.

### References

- [1] E. Wigner and H.B. Huntington, *J. Chem. Phys.* 3 (1935) 764.
- [2] N.W. Ashcroft, *Phys. Rev. Lett.* 21 (1968) 1748.
- [3] D.A. Papaconstantopoulos and B.M. Klein, *Ferroelectrics* 16 (1977) 307.
- [4] T.W. Barbee III, A. Garcia and M.L. Cohen, *Nature (London)* 340 (1989) 369.
- [5] I.F. Silvera, *Rev. Mod. Phys.* 52 (1980) 393; I.F. Silvera and R. Jochimsen, *Phys. Rev. Lett.* 43 (1979) 377.
- [6] H.K. Mao, A.P. Jephcoat, R.J. Hemley, L.W. Finger, C.S. Zha, R.M. Hazen and D.E. Cox, *Science* 239 (1988) 1131.
- [7] H.E. Lorenzana, I.F. Silvera and K.A. Goettel, *Phys. Rev. Lett.* 64 (1990) 1939.
- [8] R.J. Hemley, H.K. Mao and J.F. Shu, *Phys. Rev. Lett.* 65 (1990) 2670.
- [9] W.H. Hardy, I.F. Silvera and J.P. McTague, *Phys. Rev. B* 12 (1975) 753.
- [10] N.W. Ashcroft, *Phys. Rev. B* 41 (1990) 10963.
- [11] H.K. Mao and R.J. Hemley, *Science* 244 (1988) 1462; H.K. Mao, R.J. Hemley and M. Hanfland, *Phys. Rev. Lett.* 65 (1990) 484; M. Hanfland, R.J. Hemley and H.K. Mao, *Phys. Rev. Lett.* 70 (1993) 3760.
- [12] H. Lorenzana, I.F. Silvera and K.A. Goettel, *Phys. Rev. Lett.* 65 (1990) 1901.
- [13] D.E. Ramaker, L. Kumar and F.E. Harris, *Phys. Rev. Lett.* 34 (1975) 812.
- [14] C. Friedli and N.W. Ashcroft, *Phys. Rev. B* 16 (1977) 662.
- [15] J.H. Eggert, F. Moshary, W.J. Evans, H.E. Lorenzana, K.A. Goettel, I.F. Silvera and W.C. Moss, *Phys. Rev. Lett.* 66 (1991) 193.
- [16] A.L. Ruoff and C.A. Venderborgh, *Phys. Rev. Lett.* 66 (1991) 754.
- [17] I.F. Silvera, *Science* 247 (1990) 863; H.K. Mao and R.J. Hemley, *Science* 247 (1990) 863.
- [18] K.J. Runge, M.P. Surh, C. Mailhot and E.K. Pollock, *Phys. Rev. Lett.* 69 (1992) 3527; M.P. Suhr, T.W. Barbee III and C.M. Mailhot, *Phys. Rev. Lett.* 70 (1993) 4090.
- [19] E. Kaxiras, J. Broughton and R.J. Hemley, *Phys. Rev. Lett.* 67 (1991) 1138.
- [20] H. Nagara and T. Nakamura, *Phys. Rev. Lett.* 68 (1992) 2468.
- [21] A.A. Abrikosov, *Astron. J. (USSR)* 31 (1954) 112.
- [22] W. Kohn and L.J. Sham, *Phys. Rev. A* 140 (1965) 1133. We use the exchange-correlation expression of J. Perdew and A. Zunger, *Phys. Rev. B* 23 (1984) 5048, which is a parametrization of the exact Quantum Monte Carlo results of D.M. Ceperley and B.J. Alder, *Phys. Rev. B* 34 (1987) 2092.
- [23] R.J. Hemley, H.K. Mao, L.W. Finger, A.P. Jephcoat, R.M. Hazen and C.S. Zha, *Phys. Rev. B* 42 (1990) 6458.
- [24] A. Garcia, T.W. Barbee III, M.L. Cohen and I.F. Silvera, *Europhys. Lett.* 13 (1990) 355.
- [25] H. Chacham and S.G. Louie, *Phys. Rev. Lett.* 66 (1991) 64.
- [26] H. Chacham, X. Zhu and S.G. Louie, *Phys. Rev. Lett. B* 46 (1992) 6688.
- [27] D. Hohl, V. Natoli, D.M. Ceperley and R.M. Martin, *Phys. Rev. Lett.* 71 (1993) 541.